

## INFLUENCE OF EXERCISE HISTORY ON FALL-INDUCED HIP FRACTURE RISK

Shinya Abe<sup>1</sup>, Nathaniel Narra<sup>2</sup>, Riku Nikander<sup>3</sup>, Jari Hyttinen<sup>2</sup>, Reijo Kouhia<sup>1</sup>  
and Harri Sievänen<sup>4</sup>

Lab. Civil Engineering, Tampere University of Technology, Tampere, Finland<sup>1</sup>

Faculty of Biomedical Sciences and Engineering, BioMediTech, Tampere

University of Technology, Tampere, Finland<sup>2</sup>

Gerontology Research Center, Dept. Health Science, University of Jyväskylä,  
Jyväskylä, Finland<sup>3</sup>

The UKK Institute of Health Promotion Research, Tampere, Finland<sup>4</sup>

Hip fracture is a major public health problem. Thin superolateral cortex of the femoral neck experiences unusually high stress in a sideway fall, contributing to hip fracture risk. The aim of this study is to examine how exercise based loading history, known to affect the femoral neck cortical structure, influences fall-induced fracture risk. For this purpose, finite element models were created from the proximal femur MRI of 91 young athletic and 20 control females. Fall-induced superolateral cortical safety factors (SF) were estimated in the distal volume of femoral neck. Significantly higher ( $p < 0.05$ ) SFs were observed from femoral necks with high impact (H-I), odd impact (O-I), and repetitive impact (R-I) exercise history, indicating lower fracture risk. The results indicate that it is advisable to include some impact exercise in a fracture preventive exercise program.

**KEY WORDS:** bone strength, finite element modeling, exercise, falling, hip fracture.

**INTRODUCTION:** Hip fracture is a major public health problem leading to high rate of disability, morbidity, and even mortality in elderly population (Marks, 2010). Globally, the annual number of hip fracture and its relevant costs are estimated to reach 6.3 million and \$131.5 billion respectively by 2050 due to aging populations worldwide (Johnell, 1997). Superior cortical bone of the femoral neck is thinner than inferior region due to asymmetric loading of the dominant daily physical activity such as walking. With aging, this defect accentuates at superolateral region and can significantly contribute to hip fracture (Mayhew et al., 2005). When one falls sideways, this region experiences unusually high stress due to high impact force on lateral side of the hip. Over 90% of the hip fractures are caused by fall (Parkkari et al., 1999). If certain types of exercise can seed effective loading to this vulnerable cortical region to maintain the femoral neck strength, the hip fracture risk may decrease. Nikander et al. (2009) found that femoral necks of female athletes with a history of high impact and/or impact exercises from unusual directions have thicker cortical regions, including the superolateral cortex. However, the association of this specific exercise-induced structural adaptation with the fall-induced fracture risk has not yet been studied. Therefore, the aim of this study is to examine whether the femoral neck with a history of district exercise loading show different stress profiles in a sideways fall. For this purpose, fall-induced superolateral cortical safety factors (SF), peak nodal stress, and its location were evaluated using the finite element (FE) analysis of athletic and non-athletic femur.

**METHODS:** Proximal femur MRI data from 91 adult female athletes competing actively at national or international level and 20 habitually active, but non-competitive female control participants were used to create FE models. The study protocol was approved by the Ethics Committee of the Pirkanmaa Hospital District, and written informed consent was obtained from each participant before the study. The athletes were divided into five different groups based on the typical loading patterns of their sports (Nikander et al., 2009): high-impact (H-I: nine triple- and ten high-jumpers), odd-impact (O-I: nine soccer and ten squash players), high-magnitude (H-M: 17 power-lifters), repetitive impact (R-I: 18 endurance runners), and repetitive non-impact (R-NI: 18 swimmers). Age, body height and weight, competing career, and fall-induced impact force are given in Table 1. More group information (sport-specific training hours/week and sessions/week) are reported elsewhere (Nikander et al., 2009).

**Table 1**  
**Group Characteristics [Mean ( $\pm$ SD)]**

Group	n	Age (years)	Competing career (years)	Height (cm)	Weight (kg)	Impact force (N)
H-I	19	22.3 (4.1)	10.1 (3.4)	174 (6)	60.2 (5.4)	5101 (268)
O-I	19	25.3 (6.7)	9.6(4.8)	165 (8)	60.8 (8.3)	4991 (451)
H-M	17	27.5 (6.3)	8.0 (4.7)	158 (3)	63.3 (13.2)	4974 (532)
R-I	18	28.9 (5.6)	12.4 (6.7)	168 (5)	53.7 (3.4)	4738 (198)
R-NI	18	19.7 (2.4)	9.1 (2.6)	173 (5)	65.1 (5.6)	5285 (251)
Control	20	23.7 (3.8)	–	164 (5)	60.0 (7.4)	4944 (364)

The FE meshing and analysis of each proximal femur were performed using ANSYS 16.1 (ANSYS Inc., Houston, PA, USA). To simulate sideways falling, the femoral shaft was tilted at  $10^\circ$  with respect to the ground and the femoral neck was internally rotated by  $15^\circ$  (Figure 1). Similar boundary conditions (BCs) from a previous study (Schileo et al., 2014) were adopted in the present study (Figure 1). A 10-noded tetrahedral finite element with an element size of 1 mm was used to mesh the entire proximal femur bone geometry. On average, each bone model comprised approximately 1,600,000 elements and 2,300,000 nodes.

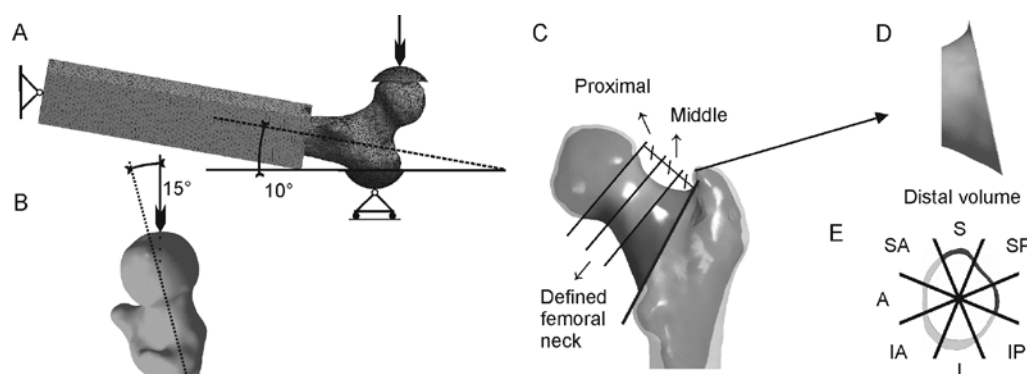


**Figure 1: Adopted BCs (A) from (Schileo et al., 2014), falling direction (A and B), defined femoral neck region and division of the femoral neck (C), the distal volume (D) and octants (E).**

The proximal femur bone was modeled as homogeneous isotropic, linear elastic materials. Young's moduli of 17 GPa and 1500 MPa (Duda et al., 1998) were set for the cortical and trabecular bone, respectively. Poisson's ratio was assumed as 0.33 for both materials. The individual impact force was estimated using the equation proposed by Bouxsein et al. (Bouxsein et al., 2007) with each participant's body height and weight (Table 1).

Regional nodal von Mises cortical stresses were obtained from the FE models. Then, mean cortical stresses were estimated for three octants in the superolateral region such as superior (S), superoposterior (SP), and posterior (P) octants in the distal volume of femoral neck (Figure 1). Then, SFs ( $<1$  indicates the failure of the material) for these octants were calculated by dividing the cortical yield limit (185 MPa) by each octant cortical stress. In the present study, SFs only in the distal volume are analyzed since it has been reported that most fractures initiate from this distal side of femoral neck (Schileo et al., 2014). More details of FE model construction from the MRI data, the adopted BCs, defining femoral neck geometry, and the octant division of the femoral neck can be found in a previous study (Abe et al., 2016). In addition, peak nodal stress and its location was determined in each model. These post-processing procedures and calculations were performed in MATLAB (MathWorks, Inc., Natick, MA, USA).

Statistical analyses were performed with SPSS 24.0 (IBM Corp., Armonk, NY, USA). Mean and SD were given as descriptive statistics. Differences in three superolateral octants' cortical SFs in the distal volume between each exercise group and the control group were estimated by multivariable analysis of covariance (MANCOVA) using the individual impact

force as a covariate. Logarithmic transformations of the octant cortical SFs and peak nodal stresses were performed prior to MANCOVA to control skewness of the data. A  $p$  value  $<0.05$  was considered statistically significant.

**RESULTS:** Figure 2 shows the unadjusted cortical SFs at S, SP, and P octants for distal femoral neck volume for each group. In the distal volume, the SP octant had lowest SFs among these three octants, which indicates this octant had the highest fracture risk. This is in line with the findings of Mayhew et al. (2005).

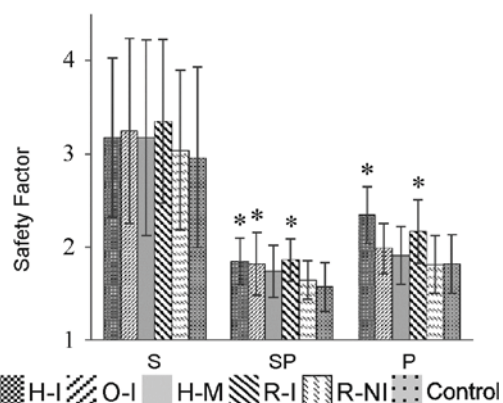


**Figure 2: Mean octant cortical stress.**  
\*shows the statistical significance  
 $p < 0.05$ .

Group	Mean (SD)	Location			
		S	SP	P	Others <sup>a</sup>
H-I	197 (33) *	5	11	0	3
O-I	206 (36)	6	11	2	0
H-M	219 (46)	5	10	2	0
R-I	180 (32) *	3	13	0	2
RN-I	219 (42)	4	11	1	2
Control	227 (44)	6	13	0	1

**Table 2. Peak nodal stress (unadjusted values in MPa) and location.**

<sup>a</sup> H-I: 2 in SP in Middle, R-I & R-NI: 2 each in S in Middle, and Control: 1 in S in Middle volume.

The H-I and R-I groups had significantly higher octant SFs ( $p < 0.05$ ) in the SP and P octants compared in the control group while the O-I group had significantly higher SF only in the SP octant. The H-I and R-I groups had significantly lower peak nodal stresses than the control group. The majority (62%) of the peak nodal stresses were located in SP octant of the distal volume (Table 2). Figure 3 shows examples of typical stress distribution from each group. Higher stresses are obviously concentrated at superolateral region, especially at its posterior side, of the distal femoral neck and the H-I, O-I, and R-I group clearly experienced lower fall-induced stress.

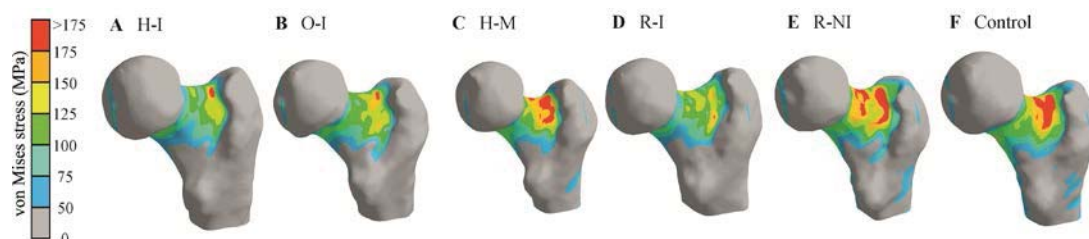


**Figure 3: Examples of typical von Mises stress distribution from each group.**

**DISCUSSION:** The significantly higher fall-induced SFs, indicating lower fracture risk, observed from the H-I and O-I groups can be explained by their specific structural adaptation of the cortical bone to impact loading. It was reported that the H-I and O-I female athletes have thicker femoral neck cortex including at the superolateral region (Nikander et al., 2009). A particularly interesting finding in the present study was that the R-I group's femoral neck also showed similar significantly higher fall-induced SFs. Rather than due to similar specific structural adaptation, positive results in the R-I are most likely attributed to the more circular shape of the femoral neck cross-section (Narra et al., 2013). A more circular bone is mechanically robust in all loading directions than an oval-shaped femoral neck which likely results from relatively decreased activity and locomotion intensity in modern humans. Physically more active medieval people had a more circular femoral neck cross-section and it

was estimated that the circular-shaped femoral neck may experience 1.3-1.5 times lower fall-induced stress than the oval-shaped femoral neck (Sievänen et al., 2007).

When the results are interpreted in the clinical context, caution is needed. As the data were obtained from young female athletes, the results may not be applied to the general population. Besides, the magnitude of impact from the H-I exercise (12-20 times BW) is clearly too risky for older people. More moderate impacts (2-4 times BW) involved in the O-I and R-I exercise regimen may provide a more feasible option to increase and/or maintain femoral neck strength among different target groups.

There are several limitations involved in this study. First, the constructed FE models were not validated against actual mechanical testing. Use of the MRI data can lead to errors due to following reasons: 1) the MR image resolution in this study was almost twice larger than ones from other QCT-based FE modeling study, and 2) inhomogeneous material properties using density data from the QCT were not applicable in this study.

**CONCLUSION:** The present results suggest that several impact loading exercises have potential to serve as a targeted exercise to strengthen the femoral neck's vulnerable region against hip fracture risk. The O-I and R-I exercises seem more feasible to general population due to their moderate impacts, and should thus be advised in the exercise program. The future study should investigate how much training load (intensity, volume, and frequency) is required to strengthen the femoral neck effectively.

#### REFERENCES:

- Abe, S., Narra, N., Nikander, R., Hyttinen, J., Kouhia, R., Sievänen, H. (2016). Exercise loading history and femoral neck strength in a sideways fall: A three-dimensional finite element modeling study. *Bone*, 92, 9–17.
- Bouxsein, M.L., Szulc, P., Munoz, F., Thrall, E., Sornay-Rendu, E., Delmas, P.D. (2007). Contribution of trochanteric soft tissues to fall force estimates, the factor of risk, and prediction of hip fracture risk. *J. Bone Miner. Res.*, 22, 825–831.
- Duda, G.N., Heller, M., Albinger, J., Schulz, O., Schneider, E., Claes, L., 1998. Influence of muscle forces on femoral strain distribution. *J. Biomech*, 31, 841–846.
- Johnell, O. (1997). The Socioeconomic Burden of Fractures: Today and in the 21st Century. *Am. J. Med*, 103, 20S–25S.
- Marks, R. (2010). Hip fracture epidemiological trends, outcomes, and risk factors, 1970-2009. *Int. J. Gen. Med*, 3, 1–17.
- Mayhew, P.M., Thomas, C.D., Clement, J.G., Loveridge, N., Beck, T.J., Bonfield, W., Burgoyne, C.J., Reeve, J. (2005). Relation between age, femoral neck cortical stability, and hip fracture risk. *Lancet*, 366, 129–135.
- Narra, N., Nikander, R., Viik, J., Hyttinen, J., Sievänen, H. (2013). Femoral neck cross-sectional geometry and exercise loading. *Clin. Physiol. Funct. Imaging*, 33, 258–266.
- Nikander, R., Kannus, P., Dastidar, P., Hannula, M., Harrison, L., Cervinka, T., Narra, N.G., Aktour, R., Arola, T., Eskola, H., Soimakallio, S., Heinonen, A., Hyttinen, J., Sievänen, H. (2009). Targeted exercises against hip fragility. *Osteoporos. Int*, 20, 1321–1328.
- Parkkari, J., Kannus, P., Palvanen, M., Natri, A., Vainio, J., Aho, H., Vuori, I., Järvinen, M. (1999). Majority of hip fractures occur as a result of a fall and impact on the greater trochanter of the femur: A prospective controlled hip fracture study with 206 consecutive patients. *Calcif. Tissue Int*, 65, 183–187.
- Schileo, E., Balistreri, L., Grassi, L., Cristofolini, L., Taddei, F. (2014). To what extent can linear finite element models of human femora predict failure under stance and fall loading configurations? *J. Biomech*, 47, 3531–3538.
- Sievänen, H., Józsa, L., Pap, I., Järvinen, M., Järvinen, T.A., Kannus, P., Järvinen, T.L. (2007). Fragile external phenotype of modern human proximal femur in comparison with medieval bone. *J. Bone Miner. Res.* 22, 537–543.